Surface effects on nanoindentation

Tong-Yi Zhang[a] and Wei-Hua Xu
Department of Mechanical Engineering, Hong Kong University of Science and Technology, Clear Water Bay, Kowloon, Hong Kong, China

(Received 4 December 2001; accepted 15 April 2002)

In this paper, we report on a study of the surface effect on nanoindentation and introduce the apparent surface stress that represents the energy dissipated per unit area of a solid surface in a nanoindentation test. The work done by an applied indentation load contains both bulk and surface work. Surface work, which is related to the apparent surface stress and the size and geometry of an indenter tip, is necessary in the deformation of a solid surface. Good agreement is found between theoretical first-order approximations and empirical data on depth-dependent hardness, indicating that the apparent surface stress plays an important role in depth-dependent hardness. In addition, we introduce a critical indentation depth. The surface deformation predominates if the indentation depth is shallower than the critical depth, while the bulk deformation predominates when the indentation depth is deeper than the critical depth.

I. INTRODUCTION

Characterizing the mechanical properties of materials at micro-/nanometer scales has become a very active area of research due to recent development of micro-/nanosystems.[1–7] Micro-/nanosystems combine mechanical, electrical, optical, and magnetic functions into microscale and even smaller scale devices to create sensors, actuators, and micro-/nanomachines. The miniaturization of electronic, optoelectronic and electromechanical devices, biosensors, and in-plants has provided the impetus for the rapid development of micro-nanosystems, nanomaterials, and micro-/nanomechanics.

At micro-/nanometer scales, materials exhibit size-dependent properties. A typical example of this size dependence is micro-/nanohardness. For instance, the hardness of (111) single-crystal Cu and cold-worked polycrystalline Cu increases from less than 1 to about 2 GPa as the indentation depth decreases from 2000 to 150 nm.[8] Similar depth-dependent hardness has been observed in a large variety of materials, such as (100) and (110) single-crystal Ag,[9] diamond-like carbon,[10] polymers, and ceramics.[3,11,12] This depth-dependent hardness has been explained with the strain-gradient plasticity by using Taylor's dislocation work hardening theory for crystalline materials and the molecular theory of yielding for polymeric materials, in which the surface effect has not been considered.[13,14] If energy dissipation on the contact surface between an indenter tip and an indented sample is considered, theoretical models will also be able to predict the size-dependent micro-nanohardness.[15,16] In this study, we seek to explore the surface effect on nanoindentation.

II. THEORY

The surface effect on nanoindentation results from the energy dissipated at the surface, which represents the work done by the indentation load against the apparent surface stress. The apparent surface stress includes two components. One is the surface stress, and the other is the pseudo-surface stress induced by friction and plastic deformation occurring at the surface. In this paper, we investigate the surface effect on nanoindentation by considering the shape and radius of an indenter tip and report on apparent surface stresses extracted from nanoindentation tests.

During indentation, the work done by an indentation load, P, can be divided into two parts: the bulk work, which is required to deform the bulk material, and the surface work, which deforms the surface of the material. This energy balance takes the following differential form:

$$P\delta h = \sigma\delta V + f\delta A \quad , \tag{1}$$

where h is the indentation depth, σ is the pressure averaged over the contact area, A, V is the volume of the indenter penetrating into the material, and f is the apparent surface stress averaged over the contact area. Rearranging Eq. (1) leads to

$$P = \sigma \frac{\delta V}{\delta h} + f \frac{\delta A}{\delta h} \quad . \tag{2}$$

[a]Address all correspondence to this author.
e-mail: mezhangt@ust.hk

The hardness, H, is defined as the ratio of the indentation load to the projected contact area, A_p:

$$H = \frac{P}{A_p} \quad . \tag{3}$$

Combining Eqs. (2) and (3) yields

$$H = \frac{\sigma}{A_p}\frac{\delta V}{\delta h} + \frac{f}{A_p}\frac{\delta A}{\delta h} \quad . \tag{4}$$

From the shape and radius of an indenter tip, we can complete the calculation of Eq. (4) for Conical, Northstar, Berkovich, and Vickers tips. We tabulate the formulas of depth-dependent hardness in Table I.

In general, σ and f are functions of the indentation depth. From Taylor's dislocation work hardening theory for crystalline materials, Nix and Gao[13] suggested that the average pressure could be expressed by $H_0\sqrt{1 + h^*/h}$, where H_0 is the hardness that would arise from the statistically stored dislocation alone, in the absence of any geometrically necessary dislocations, and h^* characterizes the depth dependence of the hardness. Lam and Chong[14] proposed an indentation model on the basis of the molecular theory of yielding for glassy polymers, in which the average pressure was expressed by $H_0(1 + \sqrt{h^*/h})$. In practice, H_0 may be regarded as the hardness when the indentation depth is sufficiently deep. However, how the apparent surface stress changes with the indentation depth has not yet been explored. To focus on the surface effect on nanoindentation, we assume that $\sigma = H_0$ and that f is a constant as the first-order approximation. If the surface effect exists, it should hold for all crystalline and amorphous materials including metals, ceramics, and polymers. Available experimental data in the literature[8,9,11,17–21] and from our laboratory[22] should therefore fit the following equations:

$$H = H_0 + \frac{f}{h[1 - h/(2R)]} \quad \text{for conical tips} \quad , \tag{5a}$$

$$H = H_0 + g\frac{f}{h} \quad \text{for Northstar, Berkovich, and Vickers tips} \quad , \tag{5b}$$

where g is a numerical factor of $2\sqrt{3}$, 1.1827, and 2.2406 for Northstar, Berkovich, and Vickers tips, respectively.

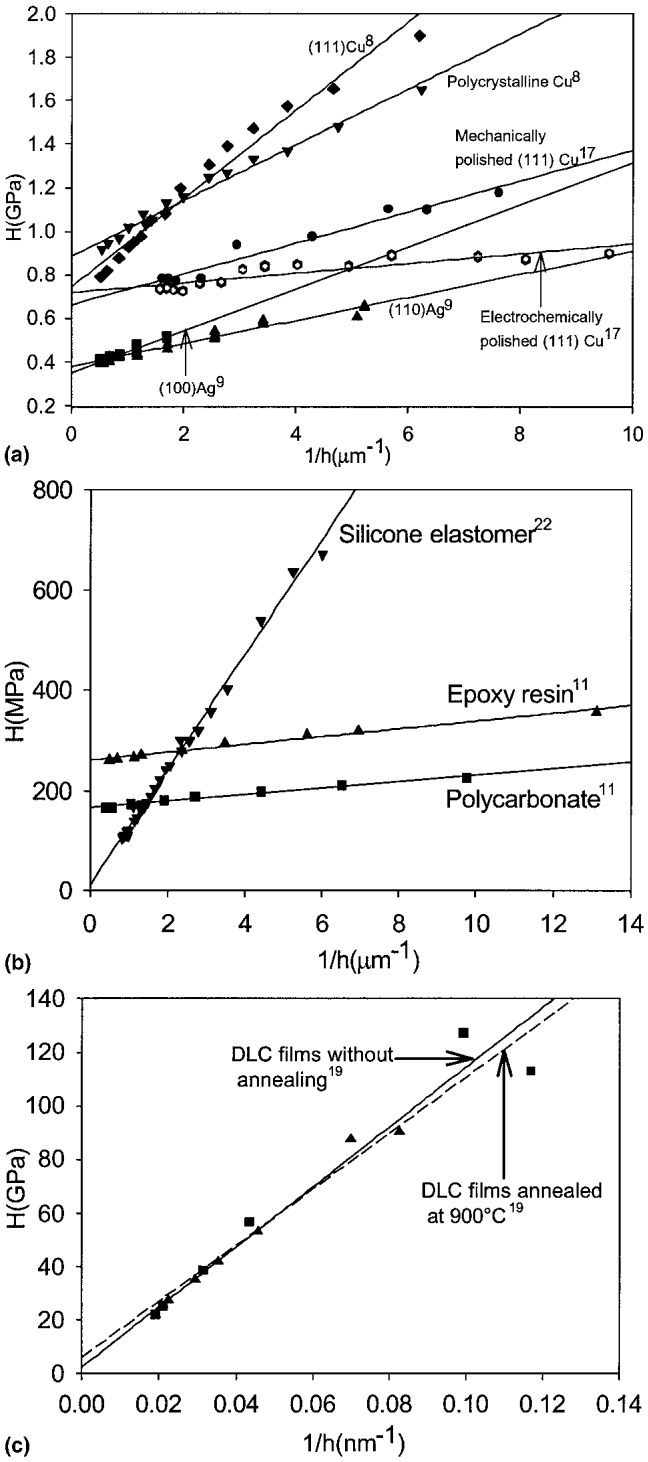

FIG. 1. Hardness versus the reciprocal indentation depth: (a) for metals; (b) for polymers; (c) for diamond-like carbon (DLC) films.

TABLE I. Hardness formulas for different indenter tips.

Tip	Radius R (nm)	Hardness formula	Remarks
Conical (Hysitron)	85, 360, 500, 1000, 1800, 5000, 20000	$H = \sigma + f/h[1 - h/(2R)]$	Depth < radius/3
Northstar (Hysitron)	30	$H = \sigma + 2\sqrt{3}\, f/h$	Sharp tip approximation
Berkovich (Hysitron)	80	$H = \sigma + 1.1827\, f/h$	Sharp tip approximation
Vickers	…	$H = \sigma + 2.2406\, f/h$	Sharp tip approximation

III. RESULTS AND DISCUSSION

Figures 1(a)–1(c) plot the depth-dependent hardness versus the reciprocal indentation depth, respectively, for metals, polymers, and diamond-like carbon (DLC) films. These plots reveal that there is a linear relationship between the hardness and the reciprocal indentation depth. This good fit is surprising because depth-dependent hardness also fits well with the formula $H = H_0\sqrt{1 + h^*/h}$ for metals[9,13] and with the formula $H = H_0(1 + \sqrt{h^*/h})$ for polymers.[11] This means that the experimental data on depth-dependent hardness can fit with different formulas derived from different models. In this communication, we focus on the surface effect and thus use Eq. (5) to fit the experimental data. The agreement between the theoretical formula and the experimental data indicates that the surface effect plays an important role in nanoindentation. The extracted values of H_0 and f are presented in Table II. It is interesting to note that the mechanically polished (111) Cu give the values of $H_0 = 0.662$ GPa and $f = 60.0$ J/m^2, whereas the electrochemically polished (111) Cu yields $H_0 = 0.718$ GPa and $f = 18.9$ J/m^2. Figure 1(a) shows that the measured hardness of the mechanical polished (111) Cu is higher than that of the electrochemically polished (111) Cu. Liu and Ngan[17] attributed this phenomenon to a work-hardened thin layer in the mechanically polished sample, as McColm[3] suggested. On the other hand, images from atomic force microscopy reveal that the surface of the mechanically polished sample is much rougher than the surface of the electrochemically polished sample. (See Figs. 1 and 2 in Ref. 17 for details.) We postulate that a rough surface may consume more energy during nanoindentation and thus lead to a higher apparent surface stress.

Figure 1(c) shows that the hardness behavior of the DLC film annealed at 900 °C is almost the same as the DLC film without annealing. The extracted values of H_0 are 6.05 and 2.44 GPa for the DLC films with and without annealing, respectively. Although the values of H_0 are so large, the hardness still strongly depends on the penetration depth for both films. For example, when the depth decreases from 50 to about 14 nm, the hardness increases from about 20 to over 90 GPa. The depth-dependent hardness may be induced by the apparent surface stress. The apparent surface stresses are 302 and 324 J/m^2, respectively, for the DLC films with and without annealing. Since the data for each film are not sufficient, we may fit all data for both films together, which yields $H_0 = 5.09$ GPa and $f = 307$ J/m^2.

Figure 2 shows the depth-dependent hardness for single crystal bcc tugsten,[20] in which we do not distinguish the diagonal directions of the Vickers indenter. When the indentation depth is less than 500 nm, the (100) nanohardness is the highest, the (110) nanohardness is in the middle, and the (111) nanohardness is the lowest. The variation in the nanohardness with the crystalline plane may indicate a difference in the apparent surface stress on the three crystalline planes. The extracted values of H_0 and f are also presented in Table II. The hardness at a sufficiently large indentation depth, H_0, is, however, more or less the same for the three crystalline planes. To understand this indentation behavior, Qiu *et al.*[23] considered the intrinsic lattice resistance, σ_0, and modified Nix and Gao's formula[13] to $H/H_0 = 3\sigma_0/H_0 + \sqrt{(1 - 3\sigma_0/H_0)^2 + h^*/h}$. As our focus is on the surface effect on nanoindentation, we will not discuss any other possible mechanisms. We believe that the results shown

TABLE II. The values of H_0 and f extracted from the nanoindentation test

Material	Indenter	H_0 (GPa)	f (J/m^2)
(110) single-crystal Ag[9]	Berkovich	0.378	44.7
(100) single-crystal Ag[9]	Berkovich	0.351	81.6
Polycrystalline Cu[8]	Berkovich	0.885	108
(111) single-crystal Cu[8]	Berkovich	0.744	172
Mechanically polished (111) Cu[17]	Berkovich	0.662	60.0
Electrochemically polished (111) Cu[17]	Berkovich	0.718	18.9
Silicon elastomer[22]	Berkovich	0.0114	97.2
Polycarbonate[11]	Berkovich	0.166	5.56
Epoxy resin[11]	Berkovich	0.261	6.54
DLC films annealed at 900 °C[19]	Northstar	6.05	302
DLC films without annealing[19]	Northstar	2.44	324
(111) single-crystal W[20]	Vickers	3.27	191
(110) single-crystal W[20]	Vickers	3.25	269
(100) single-crystal W[20]	Vickers	3.04	390
(100) single-crystal W[18]	Conical	2.88	106
(100) single-crystal Al[18]	Conical	0.110	36.8
Au film[22]	Northstar and Berkovich	0.548	44.4
1-μm-thick Al film[21]	Berkovich	0.597	18.1
2-μm-thick Al film[21]	Berkovich	0.437	15.7

in Fig. 2 indicate that the variation in the depth-dependent hardness with the crystalline plane may be caused by the anisotropic behavior of the apparent surface stress.

Figure 3 shows the depth-dependent hardness tested with different radii of conical tips, where the indentation depth was less than one-third of the radius. For (100) single-crystal A1 and (100) single-crystal W, the tip radii range from 500 to 20,000 nm and from 85 to 5000 nm, respectively. The experimental data for the (100) single-crystal W tested with the 1800-nm radius tip are not sufficient, which indicate the nanohardness to be almost independent of the penetration depth. Nevertheless, the data shown in Fig. 3 approximately exhibit the linear relationship of H with $1/\{h[1 - h/(2R)]\}$, which yields $H_0 = 2.88$ GPa and $f = 106$ J/m^2 for the (100) W and $H_0 = 0.11$ GPa and $f = 36.8$ J/m^2 for the (100) Al. These experimental results indicate that the depth- and tip radius-dependent hardness may result from the surface effect.

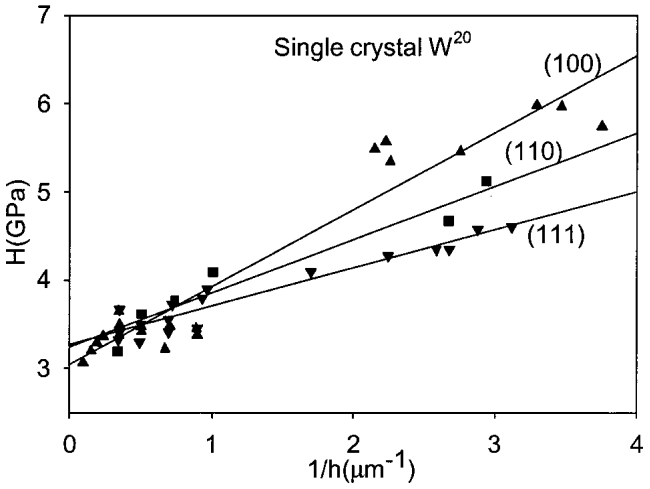

FIG. 2. Hardness versus the reciprocal indentation depth for (100), (110), and (111) W single crystals.

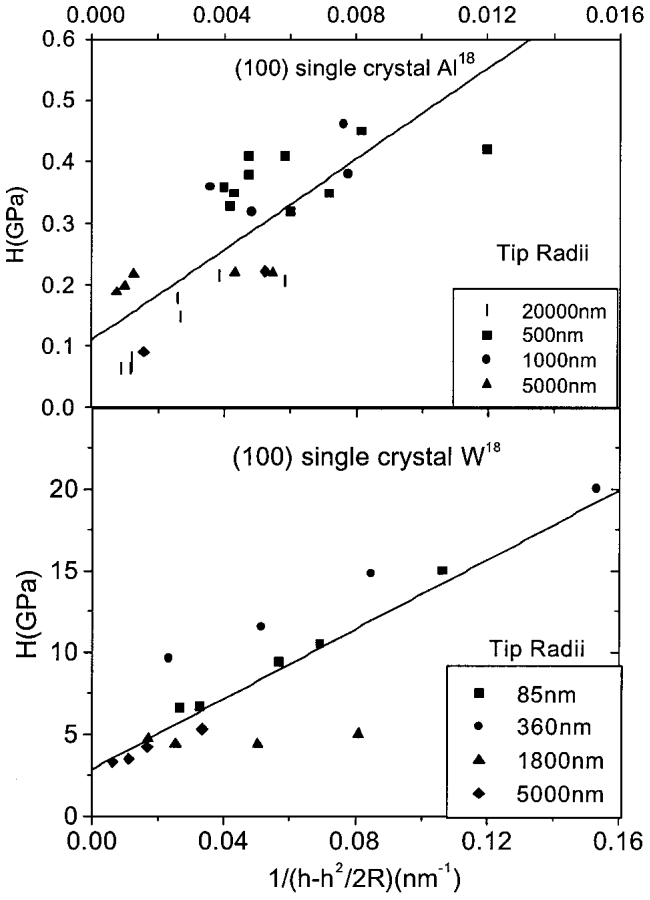

FIG. 3. Hardness tested with different radii of conical tips for (100) Al and (100) W single crystals.

Figure 4 illustrates the depth-dependent hardness of a gold film deposited on a (100) silicon wafer, of a 1-μm-thick aluminum film deposited on a glass substrate and a 2-μm-thick aluminum film deposited on a glass substrate. Both Northstar and Berkovich indenters were used in the hardness test on the gold film. The deepest indentation depth was 0.66 μm, less than 20% of the gold film thickness of 3.319 μm. Bhattacharya and Nix[24] suggested that the substrate effect is negligible when the indentation depth is less than the 20% of the film thickness. The slope of the hardness over the reciprocal penetration depth is 148 GPa/μm for the Northstar tip, which is larger than the slope of 54.1 GPa/μm for the Berkovich tip, indicating tip-dependent hardness. Dividing the slopes by the corresponding numerical factor, g, we have the apparent surface stresses of 45.7 and 42.7 J/m^2, respectively, for the Berkovich and Northstar tips. The difference in the apparent surface stress tested with the two tips may be caused by experimental error. The mean of 44.4 J/m^2 is thus listed in Table II. The hardnesses at sufficiently large indentation depth, H_0, are 0.532 GPa for the Berkovich tip and 0.564 GPa for the Northstar tip, giving a mean of 0.548 GPa.

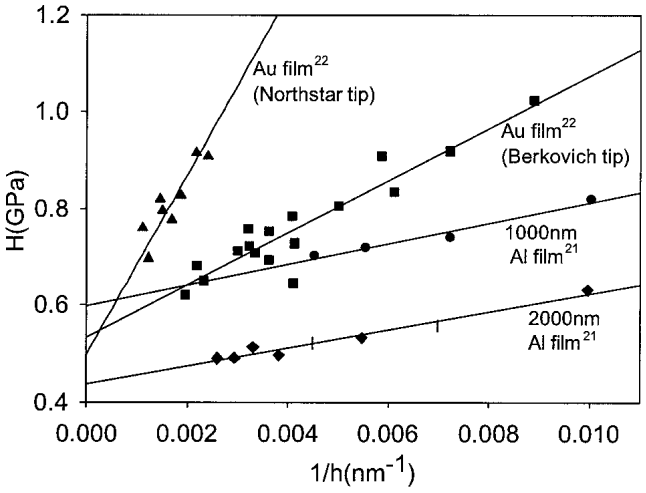

FIG. 4. Hardness of a gold film deposited on a (100) silicon wafer and for a 1-μm-thick aluminum film and a 2-μm-thick aluminum film deposited on glass substrates.

To ensure that the indentation depth is less than the 20% of the film thickness, limited data are taken from Ref. [21] and plotted in Fig. 4 for the 1- and 2-μm-thick Al films. Again, the depth-dependent hardness reveals a linear relationship with the reciprocal of the penetration depth. The slope of the hardness over the reciprocal penetration depth for the 1-μm-thick Al film is 21.4 J/m^2 (f = 18.1 J/m^2), which is almost the same as the slope of 18.6 J/m^2 (f = 15.7 J/m^2) for the 2-μm-thick Al film, indicating that the apparent surface stress may be independent of the film thickness. The results seem to be reasonable because the two films have the same deposition conditions.[21] The hardnesses at sufficiently large indentation depth, H_0, are 0.597 and 0.437 GPa, respectively, for the 1- and 2-μm-thick Al films.

Table II shows that the hard materials, such as tungsten and diamond-like carbon, have the highest hardness at sufficiently large indentation depths and the highest values of the apparent surface stresses as well. The silicon elastomer has the lowest hardness at sufficiently large indentation depth, but its apparent surface stress is much higher than the other two polymers. The polycarbonate and the epoxy resin have lower hardnesses at sufficiently large indentation depths and lower values of apparent surface stress. The values of H_0 and f for the fcc bulk metallic materials are in the middle between the hard materials and the polymeric materials.

With Nix and Gao's average pressure expression and considering the surface effect, Eq. (5) has the following forms:

$$H = H_0 \sqrt{1 + \frac{h^*}{h}} + \frac{f}{h[1 - h/(2R)]} \quad \text{for conical tips} \quad , \tag{6a}$$

$$H = H_0 \sqrt{1 + \frac{h^*}{h}} + g\frac{f}{h} \quad \text{for Northstar, Berkovich, and Vickers tips} \quad . \tag{6b}$$

Equation (6) determines the depth-dependent hardness for crystalline materials caused by work hardening in the bulk and the energy dissipation at the surface. Using Eq. (6), we can determine the predominant regions of the bulk and surface terms. For simplicity, we take Eq. (6b) as an example, which can be rewritten as

$$H = H_0 \left(1 + \sqrt{1 + \frac{h^*}{h}} - 1 + \frac{A^*}{h}\right) \qquad A^* = \frac{gf}{H_0} \quad . \tag{7}$$

Equation (7) indicates that the bulk term predominates if $\sqrt{1 + h^*/h} - 1 > A^*/h$; otherwise, the surface term predominates. Consequently, the critical depth, h_c, is given by

$$h_c = \frac{(A^*)^2}{h^* - 2A^*} \qquad h^* > 2A^* \quad . \tag{8}$$

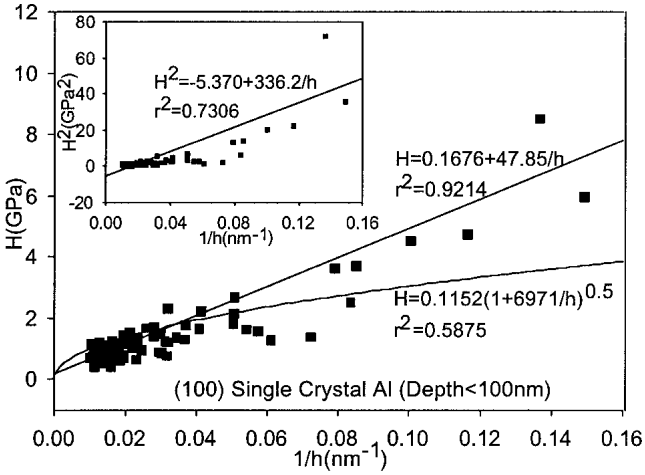

FIG. 5. Hardness versus the reciprocal indentation depth for a (100) Al single crystal, where all indentation depths are less than 100 nm. In the fitting formulas H and h are in units of GPa and nm, respectively.

The surface term predominates in the region of $h < h_c$, while the bulk term predominates in $h > h_c$. If $h^* \leqslant 2A^*$, however, the surface term will predominate over the entire region of the indentation depth. Similarly, the bulk term by Lam and Chong[14] results in a critical depth, $h_c = (A^*)^2/h^*$, for polymers. With the extracted values of h^*, H_0, and f, we estimate the value of the critical depth for various materials. For example, the mechanically and electrochemically polished (111) Cu samples have the critical depth of h_c = 75 nm and h_c = 111 nm, respectively.

To demonstrate that the surface effect predominates at the nanometer scale, we conducted nanoindentation tests with a Hysitron nanoindentation system on the standard (100) Al sample provided by the Hysitron company. Figure 5 shows the nanohardness as a function of the reciprocal of the indentation depth, where all indentation depths are smaller than 100 nm. Fitting the data with Eq. (5b) yields a correlation coefficient r^2 = 0.9214, while fitting the data with $H_0\sqrt{1 + h^*/h}$ gives a correlation coefficient r^2 = 0.5875, indicating that the depth dependence of the nanohardness is indeed controlled by the surface effect. In Fig. 5 there is a small plot of H^2 versus 1/h, which indicates that the fitting results give a meaningless negative value of $H_0{}^2$ and a low correlation coefficient, r^2 = 0.7306.

IV. CONCLUSIONS

In summary, the nanohardnesses of both crystalline and amorphous materials are approximately linearly proportional to the reciprocal of the penetration depth. In addition, at a given indentation depth, the nanohardness of the gold film tested with the Northstar tip is higher than that tested with the Berkovich tip, but the apparent surface stress is almost the same. Furthermore, the results

show that Eq. (5a) is able to predict roughly the depth- and tip radius-dependent nanohardness of the (100) W and the (100) Al. There exists a critical indentation depth. The surface effect plays a predominant role if the indentation depth is shallower than the critical depth, while the bulk deformation predominates when the indentation depth is deeper than the critical depth. However, the apparent surface stress extracted from the nanoindentation test is about 2 or 3 orders higher in magnitude than the surface energy of the same material. More theoretical and experimental studies are needed to understand the apparent surface stress and its relation to the surface morphology.

ACKNOWLEDGMENTS

This work is fully supported by a grant from the Research Grants Council of the Hong Kong Special Administrative Region of China. The authors thank Professors W.D. Nix, B.R. Lawn, and P. Tong for useful discussion.

REFERENCES

1. *Mechanical Behavior of Nanostructured Materials,* MRS Bull. **24**(2)**,** (1999) (and see articles wherein).
2. S. Suresh, Science **292,** 2447 (2001).
3. I.J. McColm, *Ceramic Hardness* (Plenum, New York, 1999).
4. T.Y. Zhang, L.Q. Chen, and R. Fu, Acta Mater. **47,** 3869 (1999).
5. W.W. Gerberich, W. Yu, D. Kramer, A. Strojny, D. Bahr, E. Lilleodden, and J. Nelson, J. Mater. Res. **13,** 421 (1998).
6. W.C. Oliver and G.M. Pharr, J. Mater. Res. **7,** 1564 (1992).
7. A. Gouldstone, K.J. Van Vliet, and S. Suresh, Nature **411,** 656 (2001).
8. K.W. McElhaney, J.J. Vlassak, and W.D. Nix, J. Mater. Res. **13,** 1300 (1998).
9. Q. Ma and D.R. Clarke, J. Mater. Res. **10,** 853 (1995).
10. H. Gao, C.H. Chiu, and J. Lee, Int. J. Solids Struct. **29,** 2471 (1992).
11. A.C.M. Chong and D.C.C. Lam, J. Mater. Res. **14,** 4103 (1999).
12. A. Krell and S. Schadlich, Mater. Sci. Eng. **A307,** 172 (2001).
13. W.D. Nix and H. Gao, J. Mech. Phys. Solids **46,** 411 (1998).
14. D.C.C. Lam and A.C.M. Chong, J. Mater. Res. **14,** 3784 (1999).
15. Y.X. Gao and H. Fan. J. Mater. Sci. (submitted for publication).
16. W.W. Gerberich, N.I. Tymiak, J.C. Grunlan, M.F. Horstemeyer, and M.I. Baskes, J. Appl. Mech. (2002, in press).
17. Y. Liu and A.H.W. Ngan, Scr. Mater. **44,** 237 (2001).
18. N.I. Tymiak, D.E. Kramer, D.F. Bahr, T.J. Wyrobek, and W.W. Gerberich, Acta Mater. **49,** 1021 (2001).
19. Data from the homepage of Hysitron Co.: www.hysitron.com/webpage2/annealin.htm.
20. N.A. Stelmashenko, M.G. Walls, L.M. Brown, and Y.V. Milman, Acta Metall. Mater. **41,** 2855 (1993).
21. R. Saha, Z. Xue, Y. Huang, and W.D. Nix, J. Mech. Phys. Solids **49,** 1997 (2001).
22. W.H. Xu, M.H. Zhao, S.Q. Shi, and T.Y. Zhang (unpublished work).
23. X. Qiu, Y. Huang, W.D. Nix, K.C. Hwang, and H. Gao, Acta Mater. **49,** 3949 (2001).
24. A.K. Bhattacharya and W.D. Nix, Int. J. Solids Struct. **24,** 1287 (1998).